

High-powered Gravitational News

Nigel T. Bishop¹, Roberto Gómez², Luis Lehner²,
Manoj Maharaj³ and Jeffrey Winicour²

¹*Department of Mathematics, Applied Mathematics and Astronomy,
University of South Africa, P.O. Box 392, Pretoria 0003, South Africa*

²*Department of Physics and Astronomy,
University of Pittsburgh, Pittsburgh, PA 15260*

³*Department of Mathematics and Applied Mathematics,
University of Durban-Westville, Durban 4000, South Africa*

Abstract

We describe the computation of the Bondi news for gravitational radiation. We have implemented a computer code for this problem. We discuss the theory behind it as well as the results of validation tests. Our approach uses the compactified null cone formalism, with the computational domain extending to future null infinity and with a worldtube as inner boundary. We calculate the appropriate full Einstein equations in computational eth form in (a) the interior of the computational domain and (b) on the inner boundary. At future null infinity, we transform the computed data into standard Bondi coordinates and so are able to express the news in terms of its standard N_+ and N_\times polarization components. The resulting code is stable and second-order convergent. It runs successfully even in the highly nonlinear case, and has been tested with the news as high as 400, which represents a gravitational radiation power of about $10^{13} M_\odot/\text{sec}$.

I. INTRODUCTION

In a series of papers in the 1960s Bondi and others [1–5] developed the theory of gravitational radiation at null infinity, and this formalism has now become accepted practice: theoretical results about gravitational radiation at future null infinity (\mathcal{I}^+) are usually expressed in terms of the Bondi news function N . However, until now it has not been possible to calculate the news numerically, except in spacetimes with special symmetries. This paper describes the theory, as well as a code, for computing the news in general (asymptotically flat) spacetimes and in regimes that include the highly nonlinear case. The code runs with the news N as large as 400 (in geometric units in which N is dimensionless). This is enormous and means that the code can cope with a power output of order $N^2 c^5 / G \approx 10^{60} W$ in conventional units. This exceeds the power that would be produced if, in 1 second, the whole Galaxy were to become gravitational radiation.

Most work in numerical relativity is done in the Cauchy “3 + 1” formalism, with the gravitational radiation estimated by perturbative methods [6–8]; these methods have not been tested on high-powered waveforms. However, here we are using the characteristic, or null cone, formalism with radial distance compactified so that \mathcal{I}^+ is contained in the (finite) grid. The theoretical foundations for this approach were laid in the 1980s [9–12]. Numerically, it has been implemented for the model problem of the scalar wave equation [14] and in general relativity under various restrictive conditions [15–18].

In a previous paper [18] we were able to compute the news in the quasi-spherical case, i.e. with the nonlinear terms in Einstein’s equations ignored. The notation and approach here follow that in [18]. The computational domain is bounded by an inner (timelike or null) worldtube, and the outer boundary of the domain is \mathcal{I}^+ . The computational domain is foliated into a sequence of null cones with initial data given on the first cone. Appropriate data on the inner boundary then enable us to use Einstein’s equations to find the spacetime geometry throughout the computational domain (see figure 1 in [18]). In addition to its other contributions, this work is also an important step towards the full implementation of Cauchy-characteristic matching as envisaged in [18] (see also [19–23]), since the characteristic code is now *complete*.

The first step in this paper is the calculation of the nonlinear terms in the Einstein equations for the Bondi-Sachs metric, and the expression of these terms in computational eth form [24,25]. This is done computationally using a symbolic programming language, and the results are described in Section II. The inner boundary of the computational domain may be a timelike, or an incoming null, worldtube, and Section III discusses the required boundary data [5]. Next, in Section IV, we investigate behavior at the outer boundary \mathcal{I}^+ . We use null cone coordinates that are defined quite generally in terms of a 2 + 1 decomposition of the inner world tube. Consequently, they do not form an inertial Bondi system at \mathcal{I}^+ . However, by carrying out a transformation to an inertial frame, we express the news in terms of the two standard polarization modes N_+ and N_\times [26]. Using computer algebra, these expressions are translated into computational eth form.

At this stage of the paper, the theoretical background for the problem has been completely specified. Section V considers various details of the numerical implementation, in particular those aspects that did not occur in the quasispherical case. We go on in Section VI to describe the results of testing the code for stability and accuracy and demonstrate that the code is second-order convergent.

We also perform a series of runs for an incoming asymmetric gravitational pulse incident on a Schwarzschild black hole. This is the fully nonlinear version of the classic black hole scattering problem first worked out in the perturbative regime [27]. As the magnitude of the pulse is ramped up various nonlinear effects become evident. The largest pulse investigated leads to a peak news of $N = 400$ for the gravitational radiation backscattered to \mathcal{I}^+ .

Some of the computational eth expressions found in this paper are quite long, and they are given in Appendices: Appendix A for the nonlinear terms in the Einstein equations, and Appendix B for the news.

II. THE NULL CONE FORMALISM

First we summarize our notation and previous results about the Einstein equations in the null cone formalism. These earlier results were complete only in the quasispherical approximation [18]. We next proceed to discuss the computer algebra techniques that were used to extend these results to the full nonlinear case in computational eth form [24], and we present the completed results.

A. Previous results

We use coordinates based upon a family of outgoing null hypersurfaces. We let u label these hypersurfaces, x^A ($A = 2, 3$), label the null rays and r be a surface area coordinate. In the resulting $x^\alpha = (u, r, x^A)$ coordinates, the metric takes the Bondi-Sachs form [1,2]

$$ds^2 = - \left(e^{2\beta} \left(1 + \frac{W}{r} \right) - r^2 h_{AB} U^A U^B \right) du^2 - 2e^{2\beta} du dr - 2r^2 h_{AB} U^B du dx^A + r^2 h_{AB} dx^A dx^B, \quad (1)$$

where W is related to the more usual Bondi-Sachs variable V by $V = r + W$; and where $h^{AB} h_{BC} = \delta_C^A$ and $\det(h_{AB}) = \det(q_{AB})$, with q_{AB} a unit sphere metric. In analyzing the Einstein equations, we also use the intermediate variable

$$Q_A = r^2 e^{-2\beta} h_{AB} U_{,r}^B. \quad (2)$$

We work in stereographic coordinates $x^A = (q, p)$ for which the unit sphere metric is

$$q_{AB} dx^A dx^B = \frac{4}{P^2} (dq^2 + dp^2), \quad (3)$$

where

$$P = 1 + q^2 + p^2. \quad (4)$$

We express q_{AB} in terms of a complex dyad q_A (satisfying $q^A q_A = 0$, $q^A \bar{q}_A = 2$, $q^A = q^{AB} q_B$, with $q^{AB} q_{BC} = \delta_C^A$ and $q_{AB} = \frac{1}{2} (q_A \bar{q}_B + \bar{q}_A q_B)$). We fix the dyad by the explicit choice

$$q^A = \frac{P}{2} (1, i) \quad (5)$$

with $i = \sqrt{-1}$. Note that we have departed from other conventions [25] to avoid factors of $\sqrt{2}$ which are awkward in numerical work. For an arbitrary Bondi-Sachs metric, h_{AB} can then be represented by its dyad component $J = h_{AB} q^A q^B / 2$, with the spherically symmetric case characterized by $J = 0$. The full nonlinear h_{AB} is uniquely determined by J , since the determinant condition implies that the remaining dyad component $K = h_{AB} q^A \bar{q}^B / 2$ satisfies $1 = K^2 - J\bar{J}$. We also introduce spin-weighted fields $U = U^A q_A$ and $Q = Q_A q^A$, as well as the (complex differential) eth operators \eth and $\bar{\eth}$. Tensor quantities and spin-weighted quantities are related as follows:

$$\begin{aligned}
h_{22} &= \frac{2}{P^2}(J + \bar{J} + 2K), \quad h_{23} = h_{32} = \frac{2}{P^2}(\bar{J} - J)i, \quad h_{33} = \frac{2}{P^2}(2K - J - \bar{J}), \\
U^2 &= \frac{P}{4}(U + \bar{U}), \quad U^3 = \frac{P}{4}(\bar{U} - U)i, \quad Q_2 = \frac{Q + \bar{Q}}{P}, \quad Q_3 = \frac{i}{P}(\bar{Q} - Q).
\end{aligned} \tag{6}$$

Refer to [24,18] for further details.

The Einstein equations $G_{\mu\nu} = 0$ decompose into hypersurface equations, evolution equations and conservation laws. In writing the field equations, we follow the formalism given in [11,12]. We find for the hypersurface equations:

$$\beta_{,r} = N_\beta, \tag{7}$$

$$U_{,r} = r^{-2}e^{2\beta}Q + N_U, \tag{8}$$

$$(r^2Q)_{,r} = -r^2(\bar{\partial}J + \partial K)_{,r} + 2r^4\bar{\partial}(r^{-2}\beta)_{,r} + N_Q, \tag{9}$$

$$W_{,r} = \frac{1}{2}e^{2\beta}\mathcal{R} - 1 - e^\beta\bar{\partial}\bar{\partial}e^\beta + \frac{1}{4}r^{-2}(r^4(\bar{\partial}\bar{U} + \bar{\partial}U))_{,r} + N_W, \tag{10}$$

where [24]

$$\mathcal{R} = 2K - \bar{\partial}\bar{\partial}K + \frac{1}{2}(\bar{\partial}^2J + \bar{\partial}^2\bar{J}) + \frac{1}{4K}(\bar{\partial}\bar{J}\bar{\partial}J - \bar{\partial}J\bar{\partial}\bar{J}). \tag{11}$$

Next, the evolution equation takes the form

$$\begin{aligned}
2(rJ)_{,ur} - \left(r^{-1}V(rJ)_{,r}\right)_{,r} = \\
-r^{-1}(r^2\bar{\partial}U)_{,r} + 2r^{-1}e^\beta\bar{\partial}^2e^\beta - (r^{-1}W)_{,r}J + N_J.
\end{aligned} \tag{12}$$

The remaining independent equations are the conservation conditions, which are discussed in Section III.

In the above equations N_β , N_U , N_Q , N_W and N_J represent the nonlinear aspherical terms (in a sense specified in [18]). Expressions for these terms are known [18] in the form of tensors and covariant derivatives, rather than complex spin-weighted fields and $\bar{\partial}$. We now calculate those nonlinear terms in the desired form.

B. New results

We have used computer algebra to calculate the nonlinear terms in two separate ways. In the first approach we start from the expressions reported previously [18]. In the second approach we start from the text-book definition of the Ricci tensor

$$R_{\mu\nu} = \partial_\alpha\Gamma_{\mu\nu}^\alpha - \partial_\nu\Gamma_{\mu\alpha}^\alpha + \Gamma_{\sigma\alpha}^\alpha\Gamma_{\mu\nu}^\sigma - \Gamma_{\sigma\nu}^\alpha\Gamma_{\mu\alpha}^\sigma. \tag{13}$$

We have checked that the two approaches gave the same results by substituting the total expressions (including the quasispherical and nonlinear parts) obtained for $\beta_{,r}$, $U_{,r}$, $Q_{,r}$, $W_{,r}$ and $J_{,ur}$ into the relevant part of the Ricci tensor, and confirming that the difference between the two results was zero.

The translation of a formula from tensor to eth formalism is ideal for computer algebra: it is straightforward and algorithmic, but lengthy. The first step is to expand any covariant derivatives in terms of partial derivatives and connection terms. Then using equation (6), each h_{AB} is expressed in terms of J , \bar{J} and K , and the U^A and Q_A are expressed in terms of U and \bar{U} , and Q and \bar{Q} , respectively. At this stage everything is in terms of spin-weighted fields, but angular derivatives of these fields are partial derivatives with respect to the coordinates. The next step is to transform these partial derivatives to \eth and $\bar{\eth}$ operators. We use simple linear algebra applied to earlier results [24] to obtain

$$A_{,q} = \frac{\eth A + \bar{\eth} A - 2ipsA}{P}, \quad A_{,p} = \frac{i(\eth A - \bar{\eth} A + 2qsA)}{P} \quad (14)$$

where A is a spin-weighted field with spin-weight s . For convenient reference we list all the spin-weighted fields that are used in the Bondi-Sachs metric and their spin-weights:

Spin-weight:	-2	-1	0	1	2
Field:	\bar{J}	\bar{Q}, \bar{U}	β, K, W	Q, U	J

Note further that the operator \eth increases the spin-weight by 1 and the operator $\bar{\eth}$ decreases the spin-weight by 1. For example, $\eth\beta$, $\eth J$ and $\eth^2\bar{U}$ all have spin-weight 1.

For quantities that are not spin-weight 0, the expressions for $A_{,q}$ and $A_{,p}$ involve q and p . However, the eth representation of geometric spin-weighted quantities (e.g. $R_{rA}q^A$) should not involve q and p , so if they appear due to one partial derivative they should be cancelled out by something else in the expression; also P should not appear in the final representation. These features provide useful checks in computer algebra calculations.

The procedures described above are complete for quantities that involve *one* angular derivative, including second derivatives involving one angular derivative and one derivative with respect to u or r . Quantities involving *two* angular derivatives are unpacked one derivative at a time, as illustrated in the example

$$\begin{aligned} W_{,qp} &= (W_{,q})_{,p} = \left(\frac{\eth W + \bar{\eth} W}{P} \right)_{,p} = \frac{P((\eth W)_{,p} + (\bar{\eth} W)_{,p}) - 2p(\eth W + \bar{\eth} W)}{P^2} \\ &= \frac{i(\eth\eth W - \eth^2 W + 2q\eth W + \bar{\eth}^2 W - \bar{\eth}\eth W - 2q\bar{\eth} W) - 2p(\eth W + \bar{\eth} W)}{P^2} \end{aligned} \quad (15)$$

We present the results of our computer algebra calculations in Appendix A. Then the complete set of null cone hypersurface and evolution equations is given by equations (7) to (12), augmented by equations (A1) to (A6). These equations are suitable for numerical implementation in computational eth form.

Most of the computer algebra was done using Maple, with some developmental work and checking on Mathematica and REDUCE. The Maple scripts are available on the World Wide Web (<http://artemis.phyast.pitt.edu/hpgnews>)

III. CONSERVATION CONDITIONS

Our discussion up to this point has only addressed the six hypersurface and evolution equations, designated by Bondi as the “main” Einstein equations [1]. They correspond to

the six components of the Ricci tensor itemized in Appendix A. Together with the equations $R_\alpha^r = 0$, they form a complete set of components of the vacuum Einstein equations. Given that the main equations are satisfied, Bondi used the Bianchi identities to show that one of these, the “trivial” equation $R_r^r = 0$, is automatically satisfied. He further showed that the remaining three equations

$$R_u^r = 0, \quad q^A R_A^r = 0. \quad (16)$$

are satisfied on a complete outgoing null cone if they are satisfied on a single spherical cross-section. By choosing this sphere to be at infinity, he identified these three equations as conservation conditions for energy and angular momentum.

In the context of our present work, we obtain a solution by requiring that these conservation conditions be satisfied on a worldtube Γ forming the inner boundary of the characteristic domain [5]. These conditions are automatically satisfied when matching across Γ to an interior solution generated, say, by Cauchy evolution. Matching is anticipated to be a primary application of the characteristic algorithm. However, in carrying out a purely characteristic evolution of the exterior, based upon data on Γ and on an initial null hypersurface, these conservation conditions must be imposed separately. This applies to the stand-alone tests of the characteristic code presented in Section VI. An alternative is to take the limit in which the worldtube collapses to a world line, in which case the conservation conditions reduce to regularity conditions at the vertices of the null cones. This approach was used in numerical evolution with an axisymmetric characteristic code [17] but would be computationally prohibitive in the 3-dimensional case.

The conservation conditions (16) dictate which metric variables can be given freely on Γ and which are subject to constraints. They contain no second r -derivatives of the metric and are the analogues, with respect to an r -foliation, of the traditional momentum constraints in a Cauchy formalism. We can therefore express them as

$$D^j(K_{ij} - \gamma_{ij}K) = 0 \quad (17)$$

in terms of the intrinsic metric γ_{ij} , the associated covariant derivative D_i and the extrinsic curvature K_{ij} in the induced coordinates $x^i = (u, x^A)$ of the worldtube Γ .

From (1), The intrinsic metric is

$$\gamma_{ij}dx^i dx^j = -e^{2\beta} \frac{V}{r} du^2 + r^2 h_{AB} (dx^A - U^A du)(dx^B - U^B du). \quad (18)$$

In analogue to the $3 + 1$ decomposition of the Cauchy formalism, a $2 + 1$ decomposition of the timelike worldtube geometry leads to the identification of $g_{AB} = r^2 h_{AB}$ as the metric of the 2-surfaces of constant u which foliate the world-tube, $e^{2\beta} V/r$ as the square of the lapse function and $(-U^A)$ as the shift vector. The extrinsic curvature of Γ is

$$K_{ij} = \delta_i^\alpha \delta_j^\beta \nabla_\alpha n_\beta \quad (19)$$

in terms of the unit normal $n_\alpha = (r/V)^{\frac{1}{2}} e^\beta \nabla_\alpha r$.

Part of the worldtube data is specification of the gauge. One simple choice is to set the shift to zero ($U^A = 0$), and the lapse to one ($V/r = e^{-2\beta}$). In this case, the components of the extrinsic curvature are

$$K_{uu} = 2\beta_{,u} + \frac{1}{2}e^{-2\beta}g_{uu,r}, \quad (20)$$

$$K_{uA} = \beta_{,A} + \frac{1}{2}e^{-2\beta}g_{uA,r}, \quad (21)$$

$$K_{AB} = \frac{1}{2}(-g_{AB,u} + e^{-2\beta}g_{AB,r}), \quad (22)$$

with

$$K = -2\beta_{,u} + \frac{2}{r}e^{-2\beta} - \frac{1}{2}e^{-2\beta}g_{uu,r}, \quad (23)$$

where g_{uu} , g_{uA} and g_{AB} are obtained from (1). It is then easy to work out the specific form of the conservation conditions using the identity

$$D^j K_{ij} = \frac{1}{\sqrt{-\gamma}}\partial_j(\sqrt{-\gamma}K_i^j) + \frac{1}{2}K_{mn}\gamma^{mn}_{,i}, \quad (24)$$

which holds for any symmetric tensor.

In order to elucidate the content of these equations we lump under the symbol \mathcal{K}_β or \mathcal{K}_A any purely null-hypersurface term (composed out of β , U^A , V and h_{AB} and their r and x^A derivatives) together with any purely worldtube term (composed out of h_{AB} and its u and x^A derivatives). Then the u -component of (17) takes the form

$$\beta_{,u} = \mathcal{K}_\beta; \quad (25)$$

and the x^A -components are

$$(e^{-2\beta}g_{uA,r} - 2\beta_{,A})_{,u} = \mathcal{K}_A, \quad (26)$$

which may be re-expressed in computational eth form as

$$Q_{,u} = -2\eth\beta_{,u} - q^A\mathcal{K}_A. \quad (27)$$

Equations (25) and (27) are generalizations to a finite worldtube of the energy and angular momentum conservation laws found by Bondi. They imply that β and Q cannot be given freely on the the worldtube but are subject to constraints. Since the worldtube values of β and Q enter as integration constants in the hypersurface equations, the evolution scheme must either update their values in accord with equations (25) and (27) or prescribe them by matching to an interior solution. (In the test cases presented in Section VI we match to an analytic interior solution). The remaining integration constants can then be posed freely on the worldtube. This gives the formal result (in our present choice of gauge) that specification of h_{AB} on the initial null hypersurface and on the worldtube and specification of β and Q on the initial slice of the worldtube determine the future evolution of the system in the region outside the worldtube.

A similar nullcone-worldtube evolution scheme holds for a general choice of lapse and shift, although the detailed equations are considerably more complicated. An example where the worldtube is null is presented in Section VII.

IV. NULL INFINITY

The spacetime can be conformally compactified in terms of the metric $d\hat{s}^2 = \ell^2 ds^2$, where $\ell = 1/r$. In (u, ℓ, x^A) coordinates, it takes the form

$$d\hat{s}^2 = - (e^{2\beta} V \ell^3 - h_{AB} U^A U^B) du^2 + 2e^{2\beta} du d\ell - 2h_{AB} U^B du dx^A + h_{AB} dx^A dx^B. \quad (28)$$

Here ℓ is a conformal factor with future null infinity \mathcal{I}^+ given by $\ell = 0$. The physical quantities governing the total energy and radiation power from the system are constructed from the leading coefficients (functions of u and x^A) in an expansion of the metric in powers of ℓ , in accord with asymptotic flatness at \mathcal{I}^+ . The coefficients H , H_{AB} , c_{AB} and L^A which enter the construction of the news function are defined by the expansions, $\beta = H + O(\ell^2)$, $h_{AB} = H_{AB} + \ell c_{AB} + O(\ell^2)$, $U^A = L^A + 2\ell e^{2H} H^{AB} D_B H + O(\ell^2)$ and $\ell^2 V = D_A L^A + \ell e^{2H} (\mathcal{R}/2 + 2D_A D^A H + 4D_A H D^A H) + O(\ell^2)$. (Note here that we have related some of the expansion coefficients by using the asymptotic content of the Einstein equations).

A. The News

The gauge freedom in the conformal metric $d\hat{s}^2$ is fixed by the gauge conditions adopted on the inner worldtube Γ . In order to construct the news function, it is convenient to refer to a conformal Bondi frame [5] with metric $d\tilde{s}^2 = \Omega^2 ds^2 = \omega^2 d\hat{s}^2$, with $\Omega = \omega\ell$, which satisfies the gauge requirements that $Q_{AB} := \tilde{g}_{AB}|_{\mathcal{I}^+} = \omega^2 H_{AB}$ is intrinsically a unit sphere metric at \mathcal{I}^+ and that $\tilde{g}^{\alpha\beta} \nabla_\alpha \Omega \nabla_\beta \Omega = O(\Omega^2)$. The conformal Bondi frame corresponds to an asymptotically Minkowskian inertial frame. Reference [13] discusses the calculation of the news in an arbitrary conformal frame relative to that in a Bondi frame.

\mathcal{I}^+ is geometrically a null hypersurface with null vector tangent to its generators given by $\tilde{n}^\alpha = \tilde{g}^{\alpha\beta} \nabla_\beta \Omega|_{\mathcal{I}^+}$ or, equivalently, $\hat{n}^\alpha = \hat{g}^{\alpha\beta} \nabla_\beta \ell|_{\mathcal{I}^+}$, with $\tilde{n}^\alpha = \omega^{-1} \hat{n}^\alpha$. In order to complete a basis for tangent vectors to \mathcal{I}^+ , let Q^α be a complex field in the neighborhood of \mathcal{I}^+ satisfying $Q^\alpha \nabla_\alpha \Omega = O(\Omega)$, $\tilde{g}_{\alpha\beta} Q^\alpha Q^\beta = O(\Omega)$ and $\tilde{g}_{\alpha\beta} Q^\alpha \bar{Q}^\beta = 2 + O(\Omega)$. In the conformal Bondi frame, the news function can then be expressed in the form [28]

$$N = \frac{1}{2\Omega} Q^\alpha Q^\beta \tilde{\nabla}_\alpha \tilde{\nabla}_\beta \Omega \quad (29)$$

evaluated in the limit of \mathcal{I}^+ . (Our conventions are chosen so that the news reduces to Bondi's original expression in the axisymmetric case [1]). In terms of the $\hat{g}_{\alpha\beta}$ frame, with conformal factor $\hat{\Omega} = \Omega/\omega = \ell$, we then have

$$N = \frac{1}{2} Q^\alpha Q^\beta \left(\frac{\hat{\nabla}_\alpha \hat{\nabla}_\beta \hat{\Omega}}{\hat{\Omega}} - \omega \hat{\nabla}_\alpha \hat{\nabla}_\beta \frac{1}{\omega} \right). \quad (30)$$

We can determine ω on \mathcal{I}^+ in the $\hat{g}_{\alpha\beta}$ frame by solving the elliptic equation governing the conformal transformation of the curvature scalar intrinsic to the 2-geometry of a $u = \text{constant}$ slice of \mathcal{I}^+ ,

$$\mathcal{R} = 2(\omega^2 + H^{AB} D_A D_B \log \omega), \quad (31)$$

where \mathcal{R} is defined in equation (11). The condition that $\tilde{g}^{\alpha\beta}\nabla_\alpha\Omega\nabla_\beta\Omega = O(\Omega^2)$ is consistent with setting $\partial_\ell\omega = 0$ but gives a relation for the time dependence of ω . Noting that $\hat{g}^{\alpha\beta}\nabla_\alpha\ell\nabla_\beta\ell = e^{-2H}D_AL^A\ell + O(\ell^2)$ and that $\hat{g}^{\alpha\beta}\nabla_\beta\ell = \hat{n}^\alpha + O(\ell)$, we obtain $2\hat{n}^\alpha\nabla_\alpha\log\omega = -e^{-2H}D_AL^A$. This is used to evolve ω given a solution of (31) as initial condition.

In order to obtain an explicit expression for the news (30) in the $\hat{g}_{\alpha\beta}$ frame we need a representation of Q^β . The choice is independent of the freedom $Q^\beta \rightarrow Q^\beta + \gamma\tilde{n}^\beta$, which leaves (30) invariant. However, it is important for physical interpretation to choose the spin rotation freedom $Q^\beta \rightarrow e^{-i\alpha}Q^\beta$ to satisfy $\tilde{n}^\alpha\tilde{\nabla}_\alpha Q^\beta = O(\Omega)$, so that the polarization frame is parallelly propagated along the generators of \mathcal{I}^+ . This fixes the polarization modes determined by the real and imaginary parts of the news to correspond to those of inertial observers at \mathcal{I}^+ .

We accomplish this by introducing the dyad decomposition $h^{AB} = (m^A\bar{m}^B + \bar{m}^A m^B)/2$ and fixing the spin rotation freedom of m^A by setting

$$m^A = \left(\frac{\bar{J}}{J}\right)^{1/4} \left(q^A \sqrt{\frac{(K+1)}{2}} - \bar{q}^A J \sqrt{\frac{1}{2(K+1)}} \right), \quad (32)$$

so that $H^{AB} = (M^A\bar{M}^B + \bar{M}^A M^B)/2$ where $M^A = m^A + O(\Omega)$. Here, in order to make m^A independent of the phase of q^A (the basis vector used in the $\tilde{\nabla}$ computations), we have introduced the phase factor $e^{i\gamma} = (\bar{J}/J)^{1/4}$. Now, setting $Q^\beta = e^{-i\alpha}\omega^{-1}(0,0,M^A) + \gamma\tilde{n}^\beta$, the requirement of an inertial polarization frame, $\tilde{n}^\alpha\tilde{\nabla}_\alpha Q^\beta = O(\Omega)$, determines the time dependence of the phase α . We obtain

$$2(\partial_u + L^A\partial_A)(i\alpha + \log\omega) = +H_{AC}\bar{M}^C(\partial_u M^A + L^B\partial_B M^A - M^B\partial_B L^A) \quad (33)$$

or, eliminating the time derivative of ω ,

$$2i(\partial_u + L^A\partial_A)\alpha = D_AL^A + H_{AC}\bar{M}^C((\partial_u + L^B\partial_B)M^A - M^B\partial_B L^A). \quad (34)$$

Equation (32) introduces numerical problems in the calculation of M^A at points where $J = 0$. We avoid these by setting $M^A = e^{i\gamma}F^A$, where

$$F^A = q^A \sqrt{\frac{(K+1)}{2}} - \bar{q}^A J \sqrt{\frac{1}{2(K+1)}}, \quad (35)$$

Substituting F^A for M^A and setting $\delta = \alpha - \gamma$, equation (34) takes the regularized form

$$2i(\partial_u + L^A\partial_A)\delta = D_AL^A + H_{AC}\bar{F}^C((\partial_u + L^B\partial_B)F^A - F^B\partial_B L^A). \quad (36)$$

We can now express the ‘‘inertial’’ news (30) in the $\hat{g}_{\alpha\beta}$ frame as

$$N = \frac{1}{2}e^{-2i\alpha}\omega^{-2}M^\alpha M^\beta \left(\frac{\hat{\nabla}_\alpha\hat{\nabla}_\beta\hat{\Omega}}{\hat{\Omega}} - \omega\hat{\nabla}_\alpha\hat{\nabla}_\beta\frac{1}{\omega} \right). \quad (37)$$

with $M^\alpha = (0,0,M^A)$. An explicit calculation then leads to

$$N = \frac{1}{4}e^{-2i\delta}\omega^{-2}e^{-2H}F^A F^B \{ (\partial_u + \mathcal{L}_L)c_{AB} + \frac{1}{2}c_{AB}D_CL^C + 2\omega D_A[\omega^{-2}D_B(\omega e^{2H})] \}, \quad (38)$$

where \mathcal{L}_L denotes the Lie derivative with respect to L^A . The eth versions of these expressions are given in Appendix B.

B. Inertial coordinates

Equation (38) is an expression for the news $N(u, x^A)$ in terms of the angular coordinates x^A determined by the gauge conditions on the inner worldtube Γ . The angular coordinates y^A of inertial observers at \mathcal{I}^+ are constant along the generators of \mathcal{I}^+ , so they are related to the x^A coordinates by $\tilde{n}^\alpha \partial_\alpha y^A = 0$ or

$$(\partial_u + L^B \partial_B) y^A = 0. \quad (39)$$

We solve this equation for $y^A(u, x^B)$, with the initial condition $y^A(u_0, x^B) = x^A$, so that y^A are stereographic angular coordinates. This yields the waveform $N'(u, y^A) = N(u, x^B(u, y^A))$ measured by inertial observers in terms of the retarded time coordinate u in which the evolution is carried out.

In order to complete the transformation to inertial coordinates we reexpress u in terms of Bondi time u_B , which is an affine parameter for the generators of \mathcal{I}^+ in a Bondi frame satisfying

$$\tilde{n}^\alpha \partial_\alpha u_B = 1, \quad (40)$$

This allows us to rewrite the news as a complex function $\tilde{N}(u_B, y^A) = N'(u(u_B, y^A), y^A)$ of inertial (Bondi) coordinates on \mathcal{I}^+ .

The news can now be readily decomposed into the two standard polarization modes. First, we must reexpress the news in terms of a polarization dyad based upon standard (θ, ϕ) spherical coordinates rather than upon stereographic coordinates. The spin rotation relating the inertial dyads Q_S^A and Q_N^A (respectively belonging to the south and north stereographic patches of the stereographic coordinates y^A) and the standard dyad \tilde{Q}^A in spherical coordinates ($\tilde{Q}^A \partial_A = \partial_\theta + (i/\sin \theta) \partial_\phi$) is

$$\tilde{Q}^A = e^{-i\phi} Q_S^A, \quad (41)$$

$$\tilde{Q}^A = e^{i\phi} Q_N^A. \quad (42)$$

Since the news function has spin-weight 2, the transformation property of spin weighted fields [24] leads in each patch to the news function \mathcal{N} referred to the the dyad \tilde{Q}^A ,

$$\mathcal{N} = e^{-2i\phi} \tilde{N}_S, \quad (43)$$

$$\mathcal{N} = e^{2i\phi} \tilde{N}_N. \quad (44)$$

The decomposition of \mathcal{N} into real and imaginary parts yields the standard polarization modes

$$N_+ = \Re[\mathcal{N}] \quad (45)$$

$$N_\times = \Im[\mathcal{N}]. \quad (46)$$

V. NUMERICAL IMPLEMENTATION

In this section we describe a numerical implementation based upon a second-order accurate finite difference approximation to the equations presented in Sec II.

A. The compactified grid

We introduce a compactified radial coordinate $x = r/(R + r)$, where the scale factor R is matched to the radius of the world tube. (In the code runs described here, R is of order 1). The radial coordinate is discretized as $x_i = X + (i - 1)\Delta x$ for $i = 1 \dots N_x$, with $\Delta x = (1 - X)/(N_x - 1)$. Here setting $X = \frac{1}{2}$ corresponds to setting $r = R$ at the inner boundary of the grid. The point $x_{N_x} = 1$ lies at null infinity. The stereographic coordinate $\xi = q + ip$ is discretized by $q_j = -1 + (j - 3)\Delta$ and $p_k = -1 + (k - 3)\Delta$ for $j, k = 1 \dots N_\xi$ and $\Delta = 2/(N_\xi - 5)$. The evolution proceeds with time step Δu , subject to a CFL condition [18].

The fields J , β , Q and W are represented by their values on this rectangular grid, e.g. $J_{ijk}^n = J(u_n, x_i, q_j, p_k)$. However, for stability [18] the field U is represented by values at the midpoints $x_{i+\frac{1}{2}} = x_i + \Delta x/2$ on a radially staggered grid (so that $U_{ijk}^n = U(u_n, x_{i+\frac{1}{2}}, q_j, p_k)$). In the following discussion, it is useful to note that asymptotic flatness implies that the fields $\beta(x)$, $U(x)$, $\tilde{W}(x) = r^{-2}W(x)$ and $J(x)$ are smooth at future null infinity \mathcal{I}^+ where $x = 1$.

B. Hypersurface equations

We discretize the hypersurface equations (7) - (10) along the lines described in [18]. The only difference here, is the introduction of the nonlinear terms, which are evaluated by second order finite differences at the midpoint of the integration cell.

C. Evolution equation

The evolution equation (12) has the schematic form

$$2(rJ)_{,ur} - \left(r^{-1}V(rJ)_{,r}\right)_{,r} = \frac{J}{r}P_1 + \tilde{\mathcal{H}}, \quad (47)$$

where we have split off the term

$$\tilde{\mathcal{H}} = -r^{-1}(r^2\partial U)_{,r} + 2r^{-1}e^\beta\partial^2e^\beta - (r^{-1}W)_{,r}J + N_J - \frac{J}{r}P_1 \quad (48)$$

which contains no u -derivatives. In order to obtain an accurate global discretization, it is convenient to introduce the evolution variable $\Phi = xJ$. (Φ vanishes in the limit $r \rightarrow 0$ and is smooth at \mathcal{I}^+). With this substitution, the evolution equation becomes

$$\begin{aligned} & 2(\Phi_{,x}(1-x) + \Phi)_{,u} - \mathcal{F}_1(\Phi_{,x}(1-x) + \Phi) - \mathcal{F}_2\Phi_{,xx} \\ &= J(1-x) \left(\frac{2}{K} \Re[\bar{\Phi}_{,u}(J_{,x}K - JK_{,x})] - 8\beta_{,x}(1-x + x\tilde{W}) \right) + \tilde{\mathcal{H}}, \end{aligned} \quad (49)$$

where

$$\mathcal{F}_1 = \tilde{W}_{,x}x(1-x) + \tilde{W} \quad (50)$$

$$\mathcal{F}_2 = (1-x)^2((1-x) + x\tilde{W}). \quad (51)$$

The elementary computational cell consists of the grid points (n, i, k, l) , $(n, i \pm 1, k, l)$ and $(n, i - 2, k, l)$ on the “old” hypersurface and the points $(n + 1, i, k, l)$, $(n + 1, i - 1, k, l)$ and $(n + 1, i - 2, k, l)$ on the “new” hypersurface. We center the evaluation at the point $(n + 1/2, i - 1/2, k, l)$ and approximate the derivatives of Φ (to second order). For example, we set

$$\begin{aligned}\Phi_{,xx} &= \frac{1}{2\Delta x^2}(\Phi_i^{n+1} - 2\Phi_{i-1}^{n+1} + \Phi_{i-2}^{n+1} + \Phi_{i+1}^n - 2\Phi_i^n + \Phi_{i-1}^n), \\ \Phi_{,x} &= \frac{1}{2\Delta x}(\Phi_i^{n+1} - \Phi_{i-1}^{n+1} + \Phi_i^n - \Phi_{i-1}^n), \\ \Phi_{,u} &= \frac{1}{2\Delta u}(\Phi_i^{n+1} + \Phi_{i-1}^{n+1} - \Phi_i^n - \Phi_{i-1}^n), \\ \Phi_{,xu} &= \frac{1}{\Delta x \Delta u} \left((\Phi_i^{n+1} - \Phi_{i-1}^{n+1}) - \frac{1}{4}(\Phi_i^n - \Phi_{i-2}^n + \Phi_{i+1}^n - \Phi_{i-1}^n) \right)\end{aligned}\tag{52}$$

and

$$\tilde{\mathcal{H}} = \frac{1}{2}(\tilde{\mathcal{H}}_{i-1}^{n+1} + \tilde{\mathcal{H}}_{i+1}^n).$$

The evolution to points $(n + 1, i, k, l)$ proceeds in an outward march along the characteristics. However, the variable Φ appears in the right hand side of Eq. (49) so that it is not convenient to adopt the null parallelogram algorithm used in the quasispherical case [18]. Instead, we use a Crank-Nicholson [29] scheme to solve the finite difference version of Eq. (49) for Φ_i^{n+1} . Rather than implementing an implicit solver to obtain Φ_i^{n+1} , we use an iterative scheme that ensures second order accurate evolution. In addition, the use of 4 points on level n in the finite differencing of $\Phi_{,xu}$ in Eq. (52) introduces some numerical dissipation that stabilizes the code even in the regime of very high amplitude fields.

D. Coordinate transformations

In order to compute the waveforms N_+ and N_\times measured by inertial observers, we need to carry out the transformation from the (u, x^A) frame to the (u_B, y^A) frame. We achieve this by first transforming to the (u, y^A) and then to (u_B, y^A) , as follows.

- Angular transformation: Rather than solving the partial differential equation (39) it is more expedient to solve the ordinary differential equation

$$\frac{dx^A}{du} = L^A(u, x^B)\tag{53}$$

with the initial condition $x^A(u_0) = y^A$ and solutions written as $x^A(u, y^A)$. This tracks a given curve (the characteristic of the PDE) along which $y^A = \text{const}$ without having to track the entire congruence. Since

$$\begin{aligned}dy^A &= \partial_u y^A du + \partial_{x^B} y^A dx^B \\ &= du(\partial_u + L^B \partial_{x^B})y^A,\end{aligned}\tag{54}$$

(53) is entirely equivalent to (39).

The numerical integration of (53) is straightforward and is implemented by the centered second order accurate scheme:

$$(x_A^{n+1} - x_A^n)_i = \Delta u (L^A)_i^{(n+\frac{1}{2})}. \quad (55)$$

Since we are covering the sphere with two stereographic patches [24], care must be taken to track the $y^A = \text{const}$ curves as they pass from one patch to the other. This is accomplished by the use of a mask which assigns the patch in which the curve lies at any time step.

- Bondi time transformation: Similarly, rather than solving the partial differential equation (40), we determine the transformation to Bondi time by means of the equivalent ordinary differential equation $du/du_B = \tilde{n}^\alpha \partial_\alpha u$, where the differentiation is along the generators of \mathcal{I}^+ . Expressing the left hand side in the (u, ℓ, x^A) coordinate system, this reduces to the differential equation $du/du_B = \omega^{-1} e^{-2H}$. We set $u_B|_{u=u_0} = u_0$ as the initial condition.

Again, the integration of this equation is straightforward. We use the centered second order accurate algorithm

$$(u_B^{n+1} - u_B^n)_i = \Delta u (\omega e^{2H})_i^{(n+\frac{1}{2})}. \quad (56)$$

- Inertial news: The solution of the above equations determine $x^A(u, y^A)$ and $u(u_B, y^A)$ and thus allow an explicit transformation of the news from grid coordinates (u, x^A) to inertial coordinates (u_B, y^A) .

VI. NUMERICAL TESTS

A. Stability

Numerical experiments were carried out which confirm the *stability* of the code, subject to a CFL condition [18], in the regime where caustics and horizons do not form. The tests were based upon long term evolution of highly nonlinear initial null data with interior worldtube data corresponding to the past horizon of a Schwarzschild black hole. See Section VII for a description of the problem. Stability persists in the regime that the u -direction, along which the grid flows, becomes spacelike. This occurs routinely in the evolution of \mathcal{I}^+ , on which every tangent direction is spacelike except the null direction of the generators, $\partial_u + L^B \partial_B$. Furthermore, a test evolution of the Schwarzschild spacetime in rigidly rotating coordinates remained stable outside the velocity of light cylinder where the grid flow becomes superluminal.

B. Accuracy

We have tested the code for *accuracy* and have verified second order convergence in grid size to analytically known values in the following test beds which have been established for null codes.

In all cases, the L_2 and L_∞ norms of the difference between the analytical (F_a) and numerical (F_n) solutions was calculated for different grid resolutions. These norms were then plotted against Δx and their convergence rate calculated. For every case, a rate of at least 1.9 was measured. This procedure is illustrated in the *nonlinear axisymmetric waveforms* case.

We also checked that the relative error $|(F_n - F_a)/F_a|$ (when $F_a \neq 0$) behaved as $\kappa(\Delta x)^2$ with κ of order 1, thus establishing the accuracy of the obtained evolution. In particular, for the case of Schwarzschild in rotating coordinates, $\kappa \leq 0.7$

- Linearized Waves:

We used solutions of the linearized characteristic equations on a Minkowski background [18]. To check accuracy of the code, we chose a solution representing an outgoing wave with angular momentum $l = 6$ with a very small amplitude ($|J| \simeq 10^{-9}$). The inner boundary was set at $R = 1$. The solution was evolved numerically for $\Delta u = 0.5$ and checked to be second order convergent to the analytic linearized solution.

- Boost and rotation symmetric solutions:

A family of solutions with exact boost and rotation symmetry called SIMPLE [17] was also used to check accuracy. Because of their cylindrical symmetry they are not asymptotically flat but were used to construct an asymptotically flat solution by smoothly pasting to asymptotically flat null data outside some radius R_o . The resulting solutions provided a nonlinear test of the second order accuracy of the evolved field variables in the domain of dependence interior to R_o .

- Schwarzschild in rotating coordinates:

By the transformation $\phi \rightarrow \tilde{\phi} + \omega u$ of the azimuthal coordinate, the Schwarzschild line element in null coordinates becomes

$$ds^2 = -(1 - \frac{2m}{r} - \omega^2 r^2 \sin^2 \theta) du^2 - 2du dr + 2\omega r^2 \sin^2 \theta du d\phi + r^2 q_{AB} dx^A dx^B. \quad (57)$$

This gauge transformation gives a nontrivial value for U at \mathcal{I}^+ and thus provides a useful test bed to check that the numerically calculated wave forms remain zero. We evolved this spacetime from $u = 0$ to $u = 0.5$ with an inner boundary at $R = 3m$ (choosing $m = 1$ and $\omega = 1$). We confirmed that the news calculated at $u = 0.5$ converged to zero to second order. This also checked the accuracy of the transformation from code coordinates to inertial coordinates at \mathcal{I}^+ .

- Waveforms from perturbed Schwarzschild black holes:

The Robinson-Trautman spacetimes describe a distorted black hole emitting purely outgoing radiation. The analytic waveform can be easily calculated in the perturbative regime [18] and then compared with the results from the code. We evolved the spacetime from $u = 0$ to $u = 1$, with an inner boundary at $R = 3m$ (where the final black hole has mass $m = 1$). Second order convergence of the numerically obtained news function was confirmed under the L_1 norm.

- Nonlinear axisymmetric waveforms

The N_\times polarization mode must vanish in spacetimes with a twist-free axisymmetry (the problem originally studied by Bondi). Since our code uses stereographic coordinates, axisymmetry is not built in and numerical noise will be produced in the N_\times mode. We then studied the nonlinear scattering of an $(\ell = 2, m = 0)$ wave off a Schwarzschild black hole and determined to what order this noise converged to zero. We gave data at $u = 0$ and evolved to $u = 0.4$. The computation was performed on grids of size $N_x = 8n + 1$ by $N_\xi = 8n + 5$ (with $n \geq 5$). Figure 1 shows the plot of $\log(\|N_\times\|_{L_2})$ vs. $\log(\Delta x)$. Convergence to second order was verified by the slope of 1.99

In the next section, we further investigate this scattering problem in the nonaxisymmetric case.

C. Timing

The characteristic algorithm uses only two complex and two real unknowns (J and U and β and W , respectively). In addition, the marching structure of the algorithm allows us to carry all temporary arrays in two dimensional form. As a result, it is much more computationally efficient than Cauchy algorithms for general relativity. Of course, being a 3-dimensional algorithm, it cannot be run in any practical sense on the current generation of workstations or personal computers. On one processor of the C90 machine at the Pittsburgh Supercomputing Center, one time step takes 6 seconds for a spatial grid of 64^3 points. A physically complete run, such as the ones discussed in the next Section, takes 1 hour (running on 1 processor).

VII. NONLINEAR SCATTERING OFF A SCHWARZSCHILD BLACK HOLE

The characteristic initial value problem on an outgoing null hypersurface requires an inner boundary condition on a worldtube (or, in a limiting case, on the worldline traced out by the vertex of a null cone). Some of the worldtube boundary data correspond to gauge freedoms. As discussed in Section III, when the worldtube is timelike this is determined by the lapse and shift arising from a $2+1$ decomposition. Here we consider an example in which the inner boundary Γ consists of an ingoing nullcone. We adopt the analogue of setting the shift to zero by choosing coordinates x^A which follow the ingoing null geodesics. We foliate Γ by slices separated by constant affine parameter λ as the analogue of fixing the lapse. We then complete the specification of the inner boundary by choosing geometric data on Γ to

correspond to the ingoing $r = 2m$ surface (the past horizon) in a Schwarzschild spacetime. This determines inner boundary values satisfying the conservation conditions.

This construction also determines outgoing null coordinates: u which labels the outgoing null hypersurfaces emanating from the foliation of Γ with $u|_{\Gamma} = \lambda$, x^A which assigns stereographic coordinates to the outgoing null rays and the surface area coordinate r .

In these coordinates, the Schwarzschild line element takes the Eddington-Finkelstein form

$$ds^2 = -\left(1 - \frac{2m}{r}\right) du^2 - 2dudr + r^2 q_{AB} dx^A dx^B, \quad (58)$$

The initial data corresponds to setting $J = 0$ as null data on $u = 0$, with the boundary conditions $\beta = U^A = 0$ and $W = -2m$ on Γ (given by $r = 2m$).

We pose the nonlinear problem of gravitational wave scattering off a Schwarzschild black hole by retaining these boundary conditions on Γ (thus continuing to satisfy the conservation conditions) but choosing null data at $u = 0$ corresponding to an incoming pulse with compact support,

$$J(u = 0, r, x^A) = \begin{cases} \lambda \left(1 - \frac{R_a}{r}\right)^4 \left(1 - \frac{R_b}{r}\right)^4 \sqrt{\frac{4\pi}{2l+1}} {}_2Y_{l,m} & \text{if } r \in [R_a, R_b] \\ 0 & \text{otherwise,} \end{cases} \quad (59)$$

where ${}_2Y_{l,m}$ is the spin two spherical harmonic.

We have calculated the plus and cross components of the news function from $u = 0$ to $u = 0.2$ (fixing $l = m = 2$) for various values of λ . As expected, for small λ , the news function scales linearly. However, for larger values, the behavior of the news function shows a stronger than linear dependence on λ . This is illustrated in Figure 2, which shows the plus component of the news, rescaled as N_+/λ , versus Bondi time. For $\lambda < 10^{-2}$, the rescaled news are essentially equal. In this perturbative regime, the news results from the backscattering of the incoming pulse off the effective potential of the interior Schwarzschild black hole [27]. However, for higher values of λ the waveform behaves quite differently. Not only is its amplitude greater (up to 3 times for $\lambda = 15$) but it also reveals the nonlinear generation of additional modes at early times for the high amplitude cases. In this regime, the mass of the system is dominated by the incoming pulse, which essentially backscatters off itself in a nonlinear way.

The nonlinearity of the news function can be also seen in Figure 3, which displays N_{\times}/λ for amplitudes $\lambda = 1.5 \times 10^{-6}$ and $\lambda = 15$. If the scaling were linear, $|N_{\times}/\lambda|$ would obtain a maximum value of ≈ 4 , while in fact its maximum is ≈ 13 .

It is worth emphasizing that the plus and cross components of the news function have been obtained by evolving the system in the (u, x^A) coordinate system and then transforming to the (u_B, y^A) coordinates and to a standard Bondi conformal frame. The surface plot of the plus component of the news in the southern hemisphere at $u_B = 0.01$, given in Figure 4, illustrate the smoothness with which our algorithm accomplishes this complete transformation.

ACKNOWLEDGMENTS

We are grateful to the referee for comments that have improved the clarity of presentation. This work has been supported by the Binary Black Hole Grand Challenge Alliance, NSF PHY/ASC 9318152 (ARPA supplemented) and by NSF PHY 9510895 and NSF INT 9515257 to the University of Pittsburgh. N.T.B. and M.M. thank the Foundation for Research Development, South Africa, for financial support, and the University of Pittsburgh for hospitality. J.W. thanks the Universities of South Africa and of Durban-Westville for their hospitality. Computer time for this project has been provided by the Pittsburgh Supercomputing Center under grant PHY860023P to J.W. and by a grant from the Center for High Performance Computing of the University of Texas at Austin, to Richard Matzner.

APPENDIX A: NONLINEAR TERMS

We have the following spin-weighted expressions for the nonlinear terms in the Einstein equations:

$R_{rr} = 0$ leads to Eq. (7) for $\beta_{,r}$ with

$$N_\beta = \frac{r}{8} (J_{,r} \bar{J}_{,r} - K_{,r}^2). \quad (\text{A1})$$

$R_{rA} q^A = 0$ leads to Eq's. (8) and (9) for $U_{,r}$ and $Q_{,r}$ with

$$N_U = \frac{e^{2\beta}}{r^2} (KQ - Q - J\bar{Q}), \quad (\text{A2})$$

and

$$N_Q = r^2 \left((1 - K)(\eth K_{,r} + \eth\bar{J}_{,r}) + \eth(\bar{J}J_{,r}) + \eth(JK_{,r}) - J_{,r}\eth K + \frac{1}{2K^2}(\eth\bar{J}(J_{,r} - J^2\bar{J}_{,r}) + \eth J(\bar{J}_{,r} - \bar{J}^2J_{,r})) \right). \quad (\text{A3})$$

$R_{AB}h^{AB} = 0$ leads to Eq. (10) for $W_{,r}$ with

$$N_W = e^{2\beta} \left((1 - K)(\eth\eth\beta + \eth\beta\eth\beta) + \frac{1}{2} \left(J(\eth\beta)^2 + \bar{J}(\eth\beta)^2 \right) - \frac{1}{2} \left(\eth\beta(\eth K - \eth\bar{J}) + \eth\beta(\eth K - \eth J) \right) + \frac{1}{2} \left(J\eth^2\beta + \bar{J}\eth^2\beta \right) \right) - e^{-2\beta} \frac{r^4}{8} (2KU_{,r}\bar{U}_{,r} + J\bar{U}_{,r}^2 + \bar{J}U_{,r}^2). \quad (\text{A4})$$

$R_{AB}q^A q^B$ leads to Eq. (12) for $J_{,ur}$ with

$$N_J = N_{J1} + N_{J2} + N_{J3} + N_{J4} + N_{J5} + N_{J6} + N_{J7} + \frac{J}{r} (P_1 + P_2 + P_3 + P_4) \quad (\text{A5})$$

where

$$\begin{aligned}
N_{J1} &= -\frac{e^{2\beta}}{r} \left(K(\bar{\partial}J\bar{\partial}\beta + 2\bar{\partial}K\bar{\partial}\beta - \bar{\partial}J\bar{\partial}\beta) + J(\bar{\partial}J\bar{\partial}\beta - 2\bar{\partial}K\bar{\partial}\beta) - \bar{J}\bar{\partial}J\bar{\partial}\beta \right), \\
N_{J2} &= -\frac{1}{2} \left(\bar{\partial}J(r\bar{U}_{,r} + 2\bar{U}) + \bar{\partial}J(rU_{,r} + 2U) \right), \\
N_{J3} &= (1-K)(r\bar{\partial}U_{,r} + 2\bar{\partial}U) - J(r\bar{\partial}\bar{U}_{,r} + 2\bar{\partial}\bar{U}), \\
N_{J4} &= \frac{r^3}{2} e^{-2\beta} \left(K^2 U_{,r}^2 + 2JKU_{,r}\bar{U}_{,r} + J^2 \bar{U}_{,r}^2 \right), \\
N_{J5} &= -\frac{r}{2} J_{,r} (\bar{\partial}\bar{U} + \bar{\partial}U), \\
N_{J6} &= r \left(\frac{1}{2} (\bar{U}\bar{\partial}J + U\bar{\partial}J)(J\bar{J}_{,r} - \bar{J}J_{,r}) \right. \\
&\quad + (JK_{,r} - KJ_{,r})\bar{U}\bar{\partial}J - \bar{U}(\bar{\partial}J_{,r} - 2K\bar{\partial}KJ_{,r} + 2J\bar{\partial}KK_{,r}) \\
&\quad \left. - U(\bar{\partial}\bar{J}_{,r} - K\bar{\partial}\bar{J}J_{,r} + J\bar{\partial}\bar{J}K_{,r}) \right), \\
N_{J7} &= r(J_{,r}K - JK_{,r}) \left(\bar{U}(\bar{\partial}J - \bar{\partial}K) + U(\bar{\partial}K - \bar{\partial}\bar{J}) \right. \\
&\quad \left. + K(\bar{\partial}U - \bar{\partial}\bar{U}) + (J\bar{\partial}\bar{U} - \bar{J}\bar{\partial}U) \right), \\
P_1 &= r^2 \left(\frac{J_{,u}}{K} (\bar{J}_{,r}K - \bar{J}K_{,r}) + \frac{\bar{J}_{,u}}{K} (J_{,r}K - JK_{,r}) \right) - 8V\beta_{,r}, \\
P_2 &= e^{2\beta} \left(-2K(\bar{\partial}\bar{\partial}\beta + \bar{\partial}\beta\bar{\partial}\beta) - (\bar{\partial}\beta\bar{\partial}K + \bar{\partial}\beta\bar{\partial}K) \right. \\
&\quad \left. + \left(J(\bar{\partial}^2\beta + (\bar{\partial}\beta)^2) + \bar{J}(\bar{\partial}^2\beta + (\bar{\partial}\beta)^2) \right) + (\bar{\partial}J\bar{\partial}\beta + \bar{\partial}\bar{J}\bar{\partial}\beta) \right), \\
P_3 &= \frac{r}{2} \left((r\bar{\partial}U_{,r} + 2\bar{\partial}U) + (r\bar{\partial}\bar{U}_{,r} + 2\bar{\partial}\bar{U}) \right), \\
P_4 &= -\frac{r^4}{4} e^{-2\beta} (2KU_{,r}\bar{U}_{,r} + J\bar{U}_{,r}^2 + \bar{J}U_{,r}^2). \tag{A6}
\end{aligned}$$

APPENDIX B: CALCULATING THE NEWS IN THE ETH FORMALISM

The eth versions of the expressions needed to calculate the news via Eq. (38) are given below:

$$\begin{aligned}
H^{AB}D_AD_B \log \omega &= \frac{1}{4} (-2\bar{\partial}^2 \log \omega \bar{J} - 2\bar{\partial}^2 \log \omega J + 4\bar{\partial}\bar{\partial} \log \omega K \\
&\quad - \bar{\partial} \log \omega \bar{\partial}J\bar{J}^2 - \bar{\partial} \log \omega \bar{\partial}J\bar{J}\bar{J} - 2\bar{\partial} \log \omega \bar{\partial}\bar{J} \\
&\quad + 2\bar{\partial} \log \omega \bar{\partial}K\bar{J}K + \bar{\partial} \log \omega \bar{\partial}\bar{J}\bar{J}K + \bar{\partial} \log \omega \bar{\partial}\bar{J}JK \\
&\quad - 2\bar{\partial} \log \omega \bar{\partial}KJ\bar{J} + \bar{\partial}J\bar{\partial} \log \omega \bar{J}K + \bar{\partial}\bar{J}\bar{\partial} \log \omega JK \\
&\quad - 2\bar{\partial}K\bar{\partial} \log \omega J\bar{J} - \bar{\partial} \log \omega \bar{\partial}J\bar{J}\bar{J} - 2\bar{\partial} \log \omega \bar{\partial}\bar{J} \\
&\quad - \bar{\partial} \log \omega \bar{\partial}\bar{J}J^2 + 2\bar{\partial} \log \omega \bar{\partial}KJK), \tag{B1}
\end{aligned}$$

$$D_A U^A = (\bar{\partial}\bar{U} + \bar{\partial}U)/2, \tag{B2}$$

$$H_{AC}\bar{F}^C\partial_u F^A = (-J_{,u}\bar{J}K - J_{,u}\bar{J} + K_{,u}J\bar{J} + K_{,u}K + K_{,u})/(J\bar{J} + 2K + 2). \quad (B3)$$

For any quantity Φ having spin-weight zero,

$$U^A\partial_A\Phi = \frac{1}{2}(\bar{U}\partial\Phi + U\bar{\partial}\Phi). \quad (B4)$$

The news N is:

$$N = \frac{1}{4}e^{-2i\delta}\omega^{-1}A^{-1}(s_1 + s_2 + \frac{1}{4}(\partial\bar{U} + \bar{\partial}U)s_3 - 4\omega^{-2}s_4 + 2\omega^{-1}s_5), \quad (B5)$$

where $A = \omega e^{2\beta}$ and the terms s_1 to s_5 are:

$$s_1 = (J^2\bar{J}_{,\ell u} + J\bar{J}J_{,\ell u} - 2JKK_{,\ell u} - 2JK_{,\ell u} + 2J_{,\ell u}K + 2J_{,\ell u})/(K + 1),$$

$$\begin{aligned} s_2 = & (\partial J_{,\ell}J\bar{J}\bar{U} + 2\partial J_{,\ell}K\bar{U} + 2\partial J_{,\ell}\bar{U} + \partial\bar{J}_{,\ell}J^2\bar{U} \\ & - 2\partial K_{,\ell}JK\bar{U} - 2\partial K_{,\ell}J\bar{U} + 2\partial UJ\bar{J}K_{,\ell} - 2\partial UJ\bar{J}_{,\ell}K \\ & - 2\partial UJ\bar{J}_{,\ell} + 4\partial UKK_{,\ell} + 4\partial UK_{,\ell} + 2\partial\bar{U}J\bar{J}J_{,\ell} - 2\partial\bar{U}JKK_{,\ell} \\ & - 2\partial\bar{U}JK_{,\ell} + 4\partial\bar{U}J_{,\ell}K + 4\partial\bar{U}J_{,\ell} + \partial J_{,\ell}J\bar{J}U + 2\partial J_{,\ell}KU + 2\partial J_{,\ell}U \\ & + \partial\bar{J}_{,\ell}J^2U - 2\partial K_{,\ell}JKU - 2\partial K_{,\ell}JU + 2\partial UJ^2\bar{J}_{,\ell} - 2\partial UJKK_{,\ell} \\ & - 2\partial UJK_{,\ell} + 2\partial\bar{U}J^2K_{,\ell} - 2\partial\bar{U}JJ_{,\ell}K - 2\partial\bar{U}JJ_{,\ell})/(2(K + 1)), \end{aligned}$$

$$s_3 = (J^2\bar{J}_{,\ell} + J\bar{J}J_{,\ell} - 2JKK_{,\ell} - 2JK_{,\ell} + 2J_{,\ell}K + 2J_{,\ell})/(K + 1),$$

$$\begin{aligned} s_4 = & (\partial A\partial\omega J\bar{J} + 2\partial A\partial\omega K + 2\partial A\partial\omega - \partial A\bar{\partial}\omega JK \\ & - \partial A\bar{\partial}\omega J - \partial\omega\bar{\partial}AJK - \partial\omega\bar{\partial}AJ + \partial A\bar{\partial}\omega J^2)/(2(K + 1)), \end{aligned}$$

$$\begin{aligned} s_5 = & (2\partial^2AJ\bar{J} + 4\partial^2AK + 4\partial^2A + 2\partial^2AJ^2 - 4\partial\bar{\partial}AJK \\ & - 4\partial\bar{\partial}AJ + \partial A\partial JJ\bar{J}^2 + 2\partial A\partial J\bar{J}K + 2\partial A\partial J\bar{J} + \partial A\partial\bar{J}J^2\bar{J} \\ & + 2\partial A\partial\bar{J}JK + 2\partial A\partial\bar{J}J - 2\partial A\partial KJ\bar{J}K - 4\partial A\partial KJ\bar{J} - 4\partial A\partial KK \\ & - 4\partial A\partial K - \partial A\bar{\partial}JJ\bar{J}K + 2\partial A\bar{\partial}JK + 2\partial A\bar{\partial}J - \partial A\bar{\partial}\bar{J}J^2K \\ & + 2\partial A\bar{\partial}KJ^2\bar{J} - \partial J\bar{\partial}AJ\bar{J}K - 2\partial J\bar{\partial}AJ\bar{J} - 2\partial J\bar{\partial}AK \\ & - 2\partial J\bar{\partial}A - \partial\bar{J}\bar{\partial}AJ^2K - 2\partial\bar{J}\bar{\partial}AJ^2 + 2\partial K\bar{\partial}AJ^2\bar{J} \\ & + 4\partial K\bar{\partial}AJK + 4\partial K\bar{\partial}AJ + \partial A\bar{\partial}JJ^2\bar{J} \\ & + \partial A\bar{\partial}\bar{J}J^3 - 2\partial A\bar{\partial}KJ^2K)/(4(K + 1)). \end{aligned} \quad (B6)$$

REFERENCES

- [1] H. Bondi, M.J.G. van der Burg and A.W.K. Metzner, *Proc. R. Soc. A* **269** 21, 1962.
- [2] R.K. Sachs, *Proc. R. Soc. A* **270** 103, 1962.
- [3] R. Penrose, *Phys. Rev. Letters*, **10** 66, 1963.
- [4] E.T. Newman and R. Penrose, *J. Math. Phys.* **3**, 566, 1962.
- [5] L.A. Tamburino and J. Winicour, *Phys. Rev.* **150** 1039, 1966.
- [6] A.M. Abrahams and C.R. Evans, *Phys. Rev. D* **42** 2585, 1990.
- [7] A.M. Abrahams, S.L. Shapiro and S. A. Teukolsky, *Phys. Rev. D* **51** 4295, 1995.
- [8] A.M. Abrahams and R.H. Price, “Applying perturbation theory to numerically generated spacetimes” *Phys. Rev. D*, in press.
- [9] H. Friedrich and J.M. Stewart, *Proc. R. Soc. A* **385** 345, 1983.
- [10] R.A. Isaacson, J.S. Welling and J. Winicour, *J. Math. Phys.* **24** 1824, 1983.
- [11] J. Winicour, *J. Math. Phys.* **24** 1193, 1983.
- [12] J. Winicour, *J. Math. Phys.* **25** 2506, 1984.
- [13] J. Winicour, *Gen. Rel. and Grav.* **19** 281 (1987).
- [14] R. Gómez, J. Winicour, and R. Isaacson, *J. Comp. Phys.* **98** 11, 1992.
- [15] N.T. Bishop, C.J.S. Clarke and R.A. d’Inverno, *Class. Quantum Grav.* **7** L23, 1990.
- [16] C.J.S. Clarke and R.A. d’Inverno, *Class. Quantum Grav.* **11** 1463, 1994.
- [17] R. Gómez, P. Papadopoulos and J. Winicour, *J. Math. Phys.* **35** 4184, 1994.
- [18] N.T. Bishop, R. Gomez, L. Lehner, and J. Winicour, *Phys. Rev. D*, **54** 6153, 1996.
- [19] N.T. Bishop, In R.A. d’Inverno, editor, *Approaches to Numerical Relativity*, Cambridge, 1992. Cambridge UP.
- [20] N.T. Bishop, *Class. Quantum Grav.* **10** 333, 1993.
- [21] N.T. Bishop, R. Gómez, P.R. Holvorcem, R.A. Matzner, P. Papadopoulos, and J. Winicour, *Phys. Rev. Letters* **76** 4303, 1996.
- [22] N.T. Bishop, In R.A. Matzner, editor, *3rd Texas Workshop on 3-Dimensional Numerical Relativity*, Austin, U. of Texas, 1996.
- [23] R.A. d’Inverno and J.A. Vickers, *Phys. Rev.*, **56**, to appear (1997).
- [24] R. Gómez, L. Lehner, P. Papadopoulos and J. Winicour, *Class. Quantum Grav.* **14** 977, 1997.
- [25] R. Penrose and W. Rindler, *Spinors and Space-Time* Vol. 1, Cambridge University Press, Cambridge, 1984.
- [26] C.W. Misner, K. S. Thorne and J.A. Wheeler, *Gravitation*, W. H. Freeman and Co., San Francisco, 1973.
- [27] R.H. Price, *Phys. Rev. D* **5** 2419, 1972.
- [28] J. Winicour, in B.R. Iyer, A. Kembhavi, J. V. Narlikar and C.V. Vishveshwara, editors, *Highlights in Gravitation and Cosmology*, Cambridge, Cambridge UP, 1988.
- [29] B. Gustaffson, H. Kreiss and J. Olinger, *Time Dependent Problems and Difference Methods*, John Wiley & Sons, New York 1995.

FIGURES

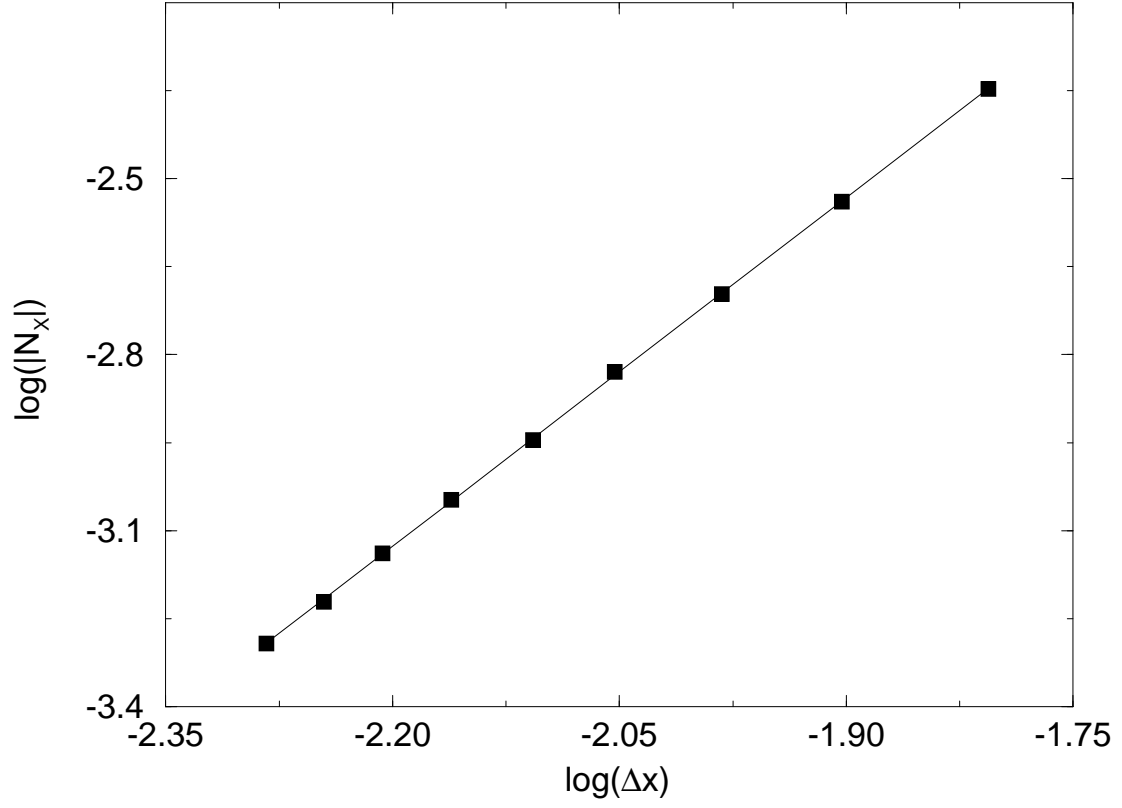


FIG. 1. The log of the L_2 norm of N_x vs. $\log(\Delta x)$. The computation was performed on grids of size $N_x = 8n + 1$ by $N_\xi = 8n + 5$ (with $5 \leq n \leq 13$). The corresponding slope is 1.99, indicating second order convergence.

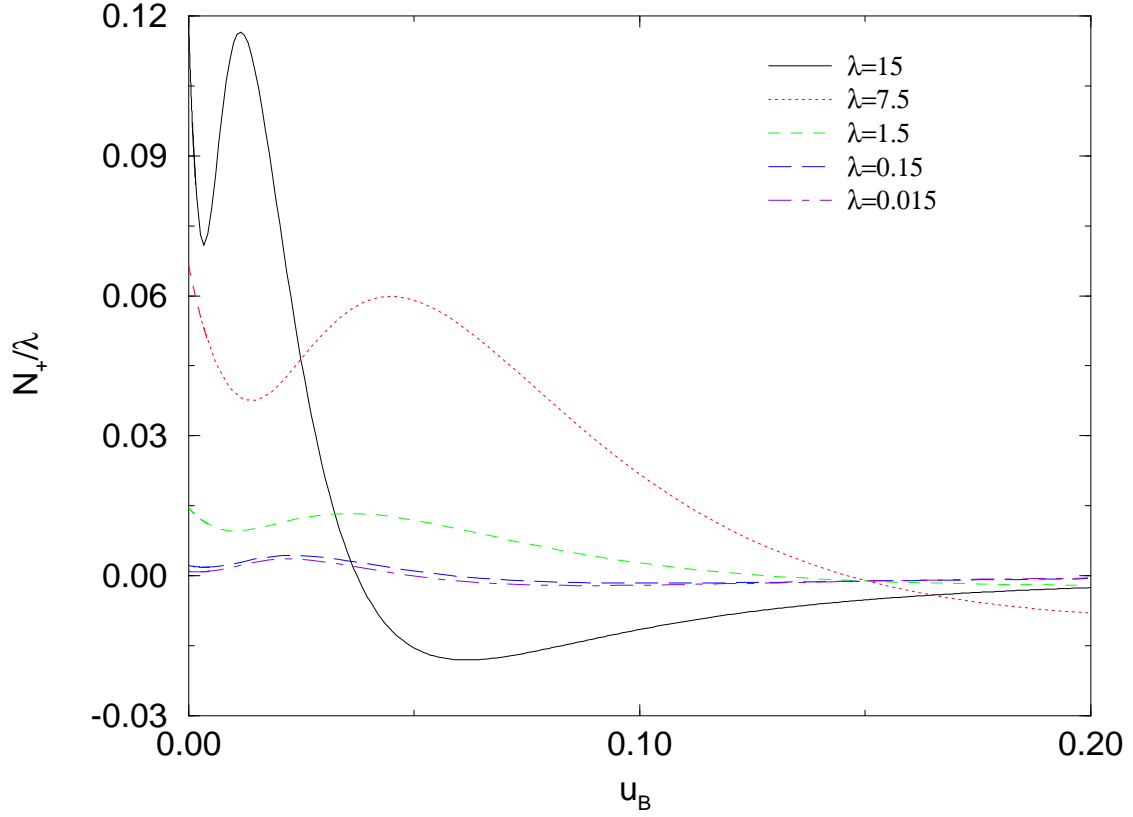


FIG. 2. Rescaled (+) component of the news for $\lambda = 1.5 \times 10^n$, with $n = -2, -1, 0, 1$, and $\lambda = 7.5$ in a ${}_2Y_{22}$ mode at $\theta = \phi = 45^\circ$. For the smallest values of λ , N_+ scales linearly with λ , while at higher values it shows significant nonlinearity which generates additional modes at early times.

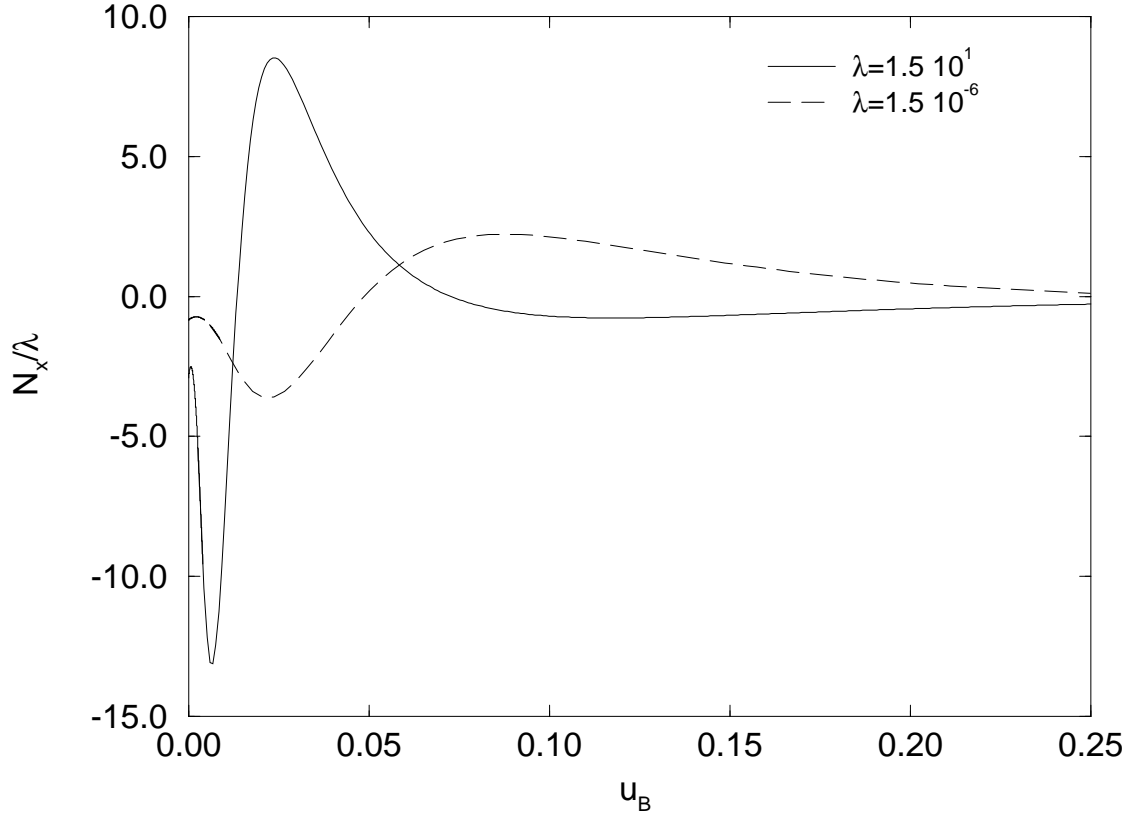


FIG. 3. Rescaled (\times) component of the news, for $\lambda = 1.5 \times 10^n$, with $n = -6$ and $n = 1$ in a ${}_2Y_{22}$ mode at $\theta = \phi = 45^\circ$. N_x/λ for $\lambda = 15$ differs by about 300% from the rescaled value for $\lambda = 1.5 \times 10^{-6}$.

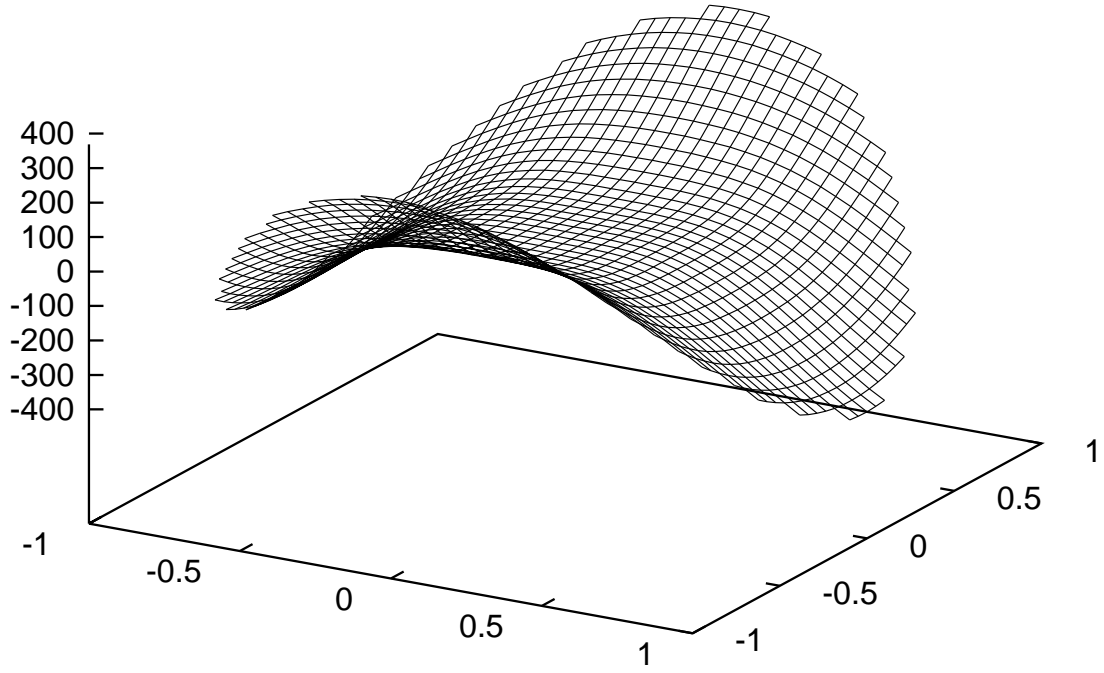


FIG. 4. Surface plot showing $N_+(u_B = 0.01, y^A)$ on the southern hemisphere. The obtained news function remains smooth after performing the sequence of transformations described in Sec. IV B which takes us from a (u, x^A) frame to a Bondi frame (u_B, y^A) .